Systematic-error-free wavefront measurement using an X-ray single-grating interferometer

Takato Inoue, Satoshi Matsuyama, Shogo Kawai, Hirokatsu Yumoto, Yuichi Inubushi, Taito Osaka, Ichiro Inoue, Takahisa Koyama, Kensuke Tono, Haruhiko Ohashi, Makina Yabashi, Tetsuya Ishikawa, and Kazuto Yamauchi

Citation: Review of Scientific Instruments **89**, 043106 (2018); doi: 10.1063/1.5026440

View online: https://doi.org/10.1063/1.5026440

View Table of Contents: http://aip.scitation.org/toc/rsi/89/4

Published by the American Institute of Physics

Systematic-error-free wavefront measurement using an X-ray single-grating interferometer

Takato Inoue,[1] Satoshi Matsuyama,[1,a)] Shogo Kawai,[1] Hirokatsu Yumoto,[2] Yuichi Inubushi,[2,3] Taito Osaka,[3] Ichiro Inoue,[3] Takahisa Koyama,[2] Kensuke Tono,[2,3] Haruhiko Ohashi,[2] Makina Yabashi,[2,3] Tetsuya Ishikawa,[3] and Kazuto Yamauchi[1,4]

[1]*Department of Precision Science and Technology, Graduate School of Engineering, Osaka University, 2-1 Yamada-oka, Suita, Osaka 565-0871, Japan*
[2]*Japan Synchrotron Radiation Research Institute, 1-1-1 Kouto, Sayo-cho, Sayo-gun, Hyogo 679-5198, Japan*
[3]*RIKEN SPring-8 Center, 1-1-1 Kouto, Sayo-cho, Sayo-gun, Hyogo 679-5148, Japan*
[4]*Center for Ultra-Precision Science and Technology, Graduate School of Engineering, Osaka University, 2-1 Yamada-oka, Suita, Osaka 565-0871, Japan*

(Received 20 February 2018; accepted 7 April 2018; published online 26 April 2018)

In this study, the systematic errors of an X-ray single-grating interferometer based on the Talbot effect were investigated in detail. Non-negligible systematic errors induced by an X-ray camera were identified and a method to eliminate the systematic error was proposed. Systematic-error-free measurements of the wavefront error produced by multilayer focusing mirrors with large numerical apertures were demonstrated at the SPring-8 Angstrom Compact free electron LAser. Consequently, wavefront aberration obtained with two different cameras was found to be consistent with an accuracy better than λ/12. *Published by AIP Publishing.* https://doi.org/10.1063/1.5026440

I. INTRODUCTION

Focusing X-rays more narrowly and densely in synchrotron radiation facilities and X-ray free electron laser (XFEL)[1,2] facilities leads to highly sensitive and high-resolution X-ray analysis. Furthermore, combining focusing optics and the excellent light sources has allowed experiments and discoveries that were impossible in the past decade. Thus, the development of X-ray focusing optical elements[3–6] is actively being promoted as an indispensable key component.

Among the various X-ray focusing optical elements, X-ray focusing mirrors are considered to be very attractive as they can focus X-rays with high reflectivity and relatively long working distances. In addition, total-reflection mirrors[6–8] can work without chromatic aberration, and multilayer mirrors[9,10] can focus quasi-monochromatic X-rays with wider energy bandwidth than other focusing optics.[3,11] Furthermore, a long footprint on an X-ray mirror makes it possible to avoid radiation damages induced by intense X-rays such as XFELs and pink beams (non-monochromatic undulator beam).[12]

Recent developments of ultraprecision machining methods[8,13–15] and metrology tools[16–19] allowed us to fabricate mirrors with shape accuracy and a surface roughness of 2 nm (peak-to-valley) and 0.2 nm (root mean square), respectively.[6] However, an important problem remains in terms of shape measurement: a precise and accurate shape measurement of large numerical aperture (NA) focusing mirrors is very difficult. This is because the tolerance of shape errors decreases with an increase in the grazing-incidence angle, which is proportional to NA. Furthermore, a steeply curved shape introduces systematic errors in metrology tools such as optical interferometers and slope profilers.[16–19] We have attempted to develop very large NA focusing mirrors for the SPring-8 Angstrom Compact free electron LAser (SACLA) that can focus XFELs down to less than 10 nm at around 9 keV. The NA and minimum curvature radius is 14.59 (11.3) mrad and 9.0 (37.0) m in the vertical (horizontal) direction, respectively. An acceptable shape error on the mirrors is less than 1 nm, according to Rayleigh's quarter-wavelength rule.[20] To the best of our knowledge, such mirrors with very large NA have never been successfully fabricated.

To overcome such difficult fabrications of X-ray optical elements, various X-ray metrologies[21–27] have been proposed. X-ray metrologies can provide information on wavefront aberrations induced by manufacturing errors and misalignments of optical elements; furthermore, they have a great advantage in that X-rays with short wavelength are very sensitive to slight wavefront distortions. In addition, substantial wavefront distortions accumulated through all optical components in a beamline can be evaluated. In this study, we focused on single-grating interferometry[28] based on the Talbot effect,[29] as an X-ray metrology. Interferometers can detect the distortion of wavefronts from the disturbance of periodical interference patterns, which is the so-called self-image. The method is highly advantageous for the following reasons: (i) The experimental setup is very simple, leading to only a few systematic errors. (ii) Rapid measurements are possible; the Fourier transform method can complete the measurement during single exposure because the setup has no moving components, and even the fringe scan method[30] requires only a few image acquisitions. (iii) This method is almost insensitive to small grating positioning errors caused by vibrations of a focusing element, grating, and incident X-ray beam, which is most important to characterize a nanobeam with a width of less

a)Author to whom correspondence should be addressed: matsuyama@prec.eng.osaka-u.ac.jp

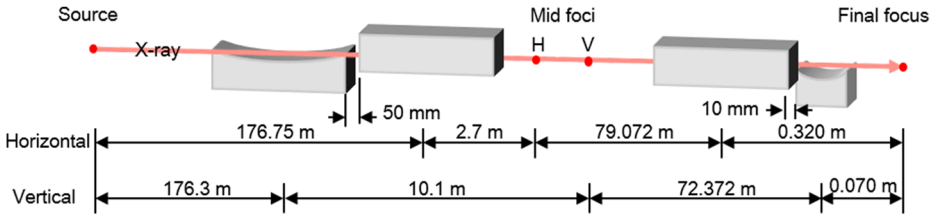

FIG. 1. Schematic of the sub-10 nm focusing system for SACLA.

than 10 nm. In addition, this is useful for an XFEL nanobeam because an XFEL beam tends to have shot-by-shot position fluctuations.[31]

Studies to measure wavefront aberrations of various optical elements using a grating interferometer have already been reported.[27,28,32] In this study, the systematic errors of a single-grating interferometer were investigated in detail. In general, metrology tools include systematic errors; one of the most important issues to be solved is how to determine and remove systematic errors. To the best of our knowledge, there is no detailed report on the systematic errors of X-ray single-grating interferometers. Therefore, systematic errors caused by a grating and using an X-ray camera were carefully investigated. Consequently, a non-negligible systematic error derived from the distortion produced by using an X-ray camera was detected. A novel method for determining systematic errors caused by using cameras was proposed. A demonstration to determine wavefront aberrations on the large NA multilayer focusing mirrors, which are under development was carried out at SACLA with a photon energy of 9.1 keV. The systematic errors obtained with different parameters and cameras were compared and discussed.

II. FOCUSING SYSTEM AND EXPERIMENTAL SETUP

A large-NA focusing system, which has been developed in EH5 at the BL3 of SACLA, was used for this research. Typical parameters of XFEL are as follows: a photon energy of 9.1 keV, a pulse energy of ~400 μJ just behind a source, a repetition rate of 30 Hz, and a pulse duration of ~8 fs.[33] The focusing system consists of two Kirkpatrick–Baez (KB) mirrors,[34] i.e., a two-stage focusing system,[35] as shown in Fig. 1 and Table I. To prepare the high-performance mirrors, quartz glass substrates were super-polished with computer-controlled elastic emission machining (EEM).[13] Subsequently, the substrates for the downstream KB mirror were covered with the Pt/C multilayer,[10,36] which has laterally graded periods (see Table II), using a DC magnetron sputtering method. Owing to the multilayer on the downstream KB mirror, the focusing system can have a NA of more than 0.01. Furthermore, the two-stage focusing system allows for a very large demagnification factor [16 176 (Horizontal) and 18 047 (Vertical)].

With regard to the experimental setup of the single-grating interferometer, a phase grating (NTT Advanced Technology Cooperation) with a phase shift of $\pi/2$ and a period of 2.5 μm was installed 11.63 mm downstream of the final focus. In addition, an X-ray camera (Hamamatsu Photonics) was installed 820 mm downstream of the focus. The magnification of the Talbot self-images on the detector was 70.5 and the period of the Talbot self-image on the detector was 176.25 μm. The dimensions of the effective bright field at the camera position were 16.4 mm and 19.4 mm in the horizontal and vertical directions, respectively. An indirect-detection X-ray camera was employed for acquiring self-images. It consists of a 10-μm-thick Gd_2O_2S scintillator, a mirror for visible light, which is arranged at an angle of 45°, two lenses, and a two-dimensional image detector. Visible light converted from X-rays by using the scintillator is transferred to the 90° direction and is guided to the detector via the two lenses. The first lens (of focal length 105 mm) is fixed to the scintillator unit, and the second lens is fixed to the detector unit. The scintillator and detector units are interchangeable. Table III shows the details of the two detectors used for comparative experiments. The effective pixel size was estimated, considering the focal length of the two lenses in the scintillator and detector units. The detectors intercepted whole of the bright field sufficiently. Since the resolution of these X-ray cameras is sufficiently higher than the period of a self-image, it can be directly recorded without Moiré fringes formed by an absorption grating, which is often employed for phase imaging with a parallel beam.[37]

All wavefront measurements were performed with a four-step fringe-scanning method.[30] Each self-image for the

TABLE I. Parameters of the sub-10 nm focusing system.

	Upstream KB mirror		Downstream KB mirror	
	Vertical focusing	Horizontal focusing	Horizontal focusing	Vertical focusing
Average grazing incidence angle (mrad)	1.51	1.51	15.7	12.6
Mirror length (mm)	400	400	380	100
Focal length from mirror center (m)	10.10	2.70	0.320	0.070
Demagnification	17.46	65.46	247.1	1033.9
Numerical aperture ($\times 10^{-3}$)	0.028	0.11	11.3	14.59
Focus size (nm, FWHM)	1995.2	507.9	4.87	3.8

TABLE II. Parameters of multilayer films.

	Horizontal focusing	Vertical focusing
Material	Pt/C	Pt/C
Number of periods	30	30
X-ray energy (keV)	9.1	9.1
Maximum d-space (nm) [grazing incidence angle (mrad)]	7.25 (22.88)	9.10 (24.68)
Minimum d-space (nm) [grazing incidence angle (mrad)]	3.12 (11.58)	2.87 (10.09)
Thickness ratio (Gamma)	0.5	0.5

TABLE III. Parameters of detector units.

	Camera A	Camera B
Device	CCD (C9300-124)	CMOS (ORCA-Flash4.0)
Pixel number	4000 × 2672	2048 × 2048
Pixel size (μm)	9.0 × 9.0	6.5 × 6.5
Effective pixel size (μm)	9.0 × 9.0	13.65 × 13.65
Focal length (mm)	105	50
F number	4.2	2.0

fringe-scan method was acquired by integrating 30 XFEL shots. A general reconstruction protocol was employed.[30] After the reconstruction of the wavefront shape, the quadratic function, which indicates the defocus component, was subtracted from the wavefront shape. Furthermore, the coma aberration caused by an incidence angle error of the focusing mirror[38] was subtracted. Then, the component left is expressed as the wavefront aberration. The coma aberration function was experimentally obtained by accurately varying the incident angle. The shape of the coma aberration was in good agreement with simulation results based on Fresnel–Kirchhoff's diffraction theory.[39] The repeatability of the wavefront measurements is 0.2 rad (root mean squared: rms), which is sufficiently good. This error comes from the shot-to-shot intensity modulation of XFEL pulses. In the same experiments performed at SPring-8, the repeatability was 0.096 rad (rms).

III. SYSTEMATIC ERRORS OF A SINGLE GRATING INTERFEROMETER

We carefully examined the systematic errors of the single-grating interferometer. Since it is a simple setup, it is assumed that the errors result from only the manufacturing error of the grating and the components of an X-ray camera. The experiments to evaluate the errors were carried out using the setup shown in Fig. 1 at the BL3 (EH5) of SACLA.

First, a systematic error derived from the grating was investigated by changing the irradiation area of the grating along the grating plane because unwanted distribution of a grating period can introduce artificial wavefront distortions. As shown in Fig. 2, the in-plane measurements were performed at five positions at a 300 μm pitch. The difference of the obtained wavefront aberrations from the average is plotted on a graph in Fig. 2. Here, the horizontal axes of the graph, that represent the position on the camera, were normalized by the width of the self-image at the camera position. Peak-to-valley height and rms of the differences were 1.0 rad and

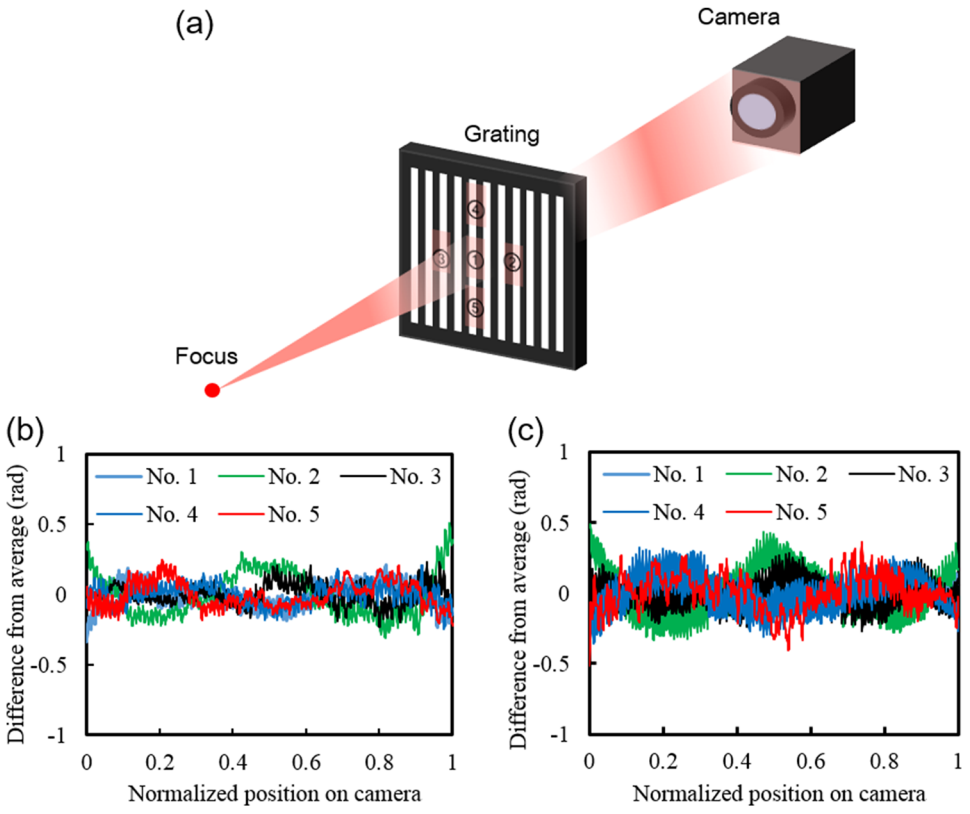

FIG. 2. Wavefront aberrations depending on the irradiation position along the grating plane. (a) Positions of irradiation on the grating and the differences of wavefront aberration at these spots, in the (b) vertical and (c) horizontal dimensions.

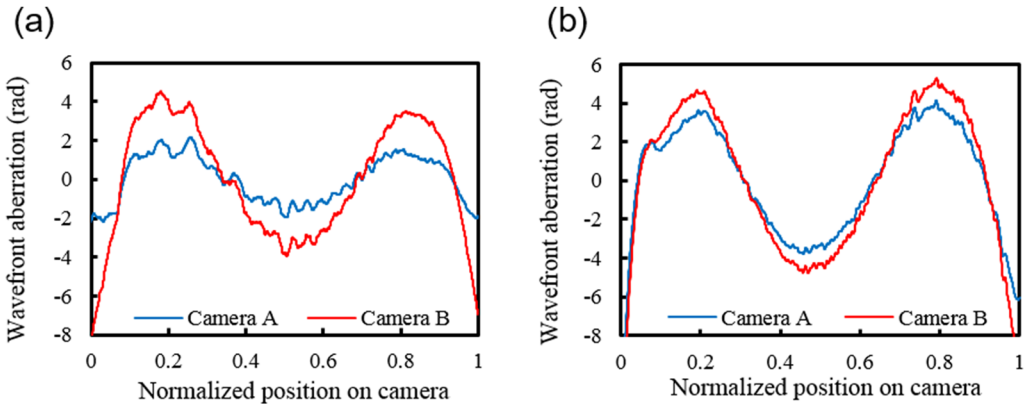

FIG. 3. Wavefront aberrations obtained with different cameras. (a) Vertical and (b) horizontal.

0.17 rad, respectively, which is much less than λ/4. Thus, it was confirmed that the systematic error derived from the grating hardly affects the determination of wavefront aberrations. This result implies that the grating was perfectly fabricated with a period uniformity of at least 6 nm, which can be attributed to the fact that the electron beam lithography system exposed a 400-μm area of the grating, which is larger than the used area [262.8 μm (H) × 339.5 μm (V)] on the grating in the experimental setup.

Next, the systematic error derived from the camera was investigated. Two different X-ray cameras (A, B) were used, and the results of wavefront measurements obtained by each camera are compared in Fig. 3. It was found that the obtained wavefront aberrations are different. Particularly in the vertical direction, there was a difference of more than 2.0 rad. This result indicates that the systematic error derived from the camera cannot be ignored. The distortions of the lenses and the mirrors and the pixel-size nonuniformity of the image detectors may cause the systematic errors.

IV. SYSTEMATIC-ERROR-FREE WAVEFRONT MEASUREMENT METHOD

We proposed a novel method to determine and remove systematic errors from a camera system. In this method, a camera is scanned one-dimensionally and wavefront measurements are performed at each position. If a camera has a systematic error, an inconsistency among all the wavefront data is observed. In order to extract this inconsistency, we employed the following algorithm. If the camera is scanned in the x-direction, a measured wavefront value at the (m, n) pixel on the camera can be expressed as

$$\varphi_{meas}(x, m, n) = \varphi_{real}(m, n) + \varphi_{sys}(m, n), \tag{1}$$

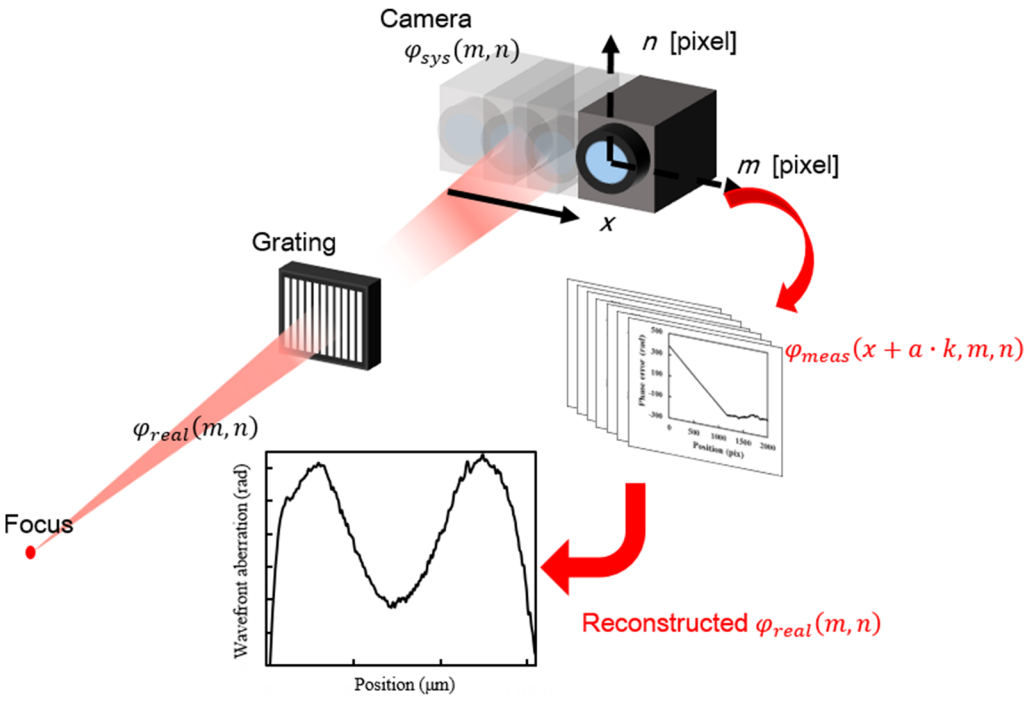

FIG. 4. Schematic to determine and remove systematic errors from a camera.

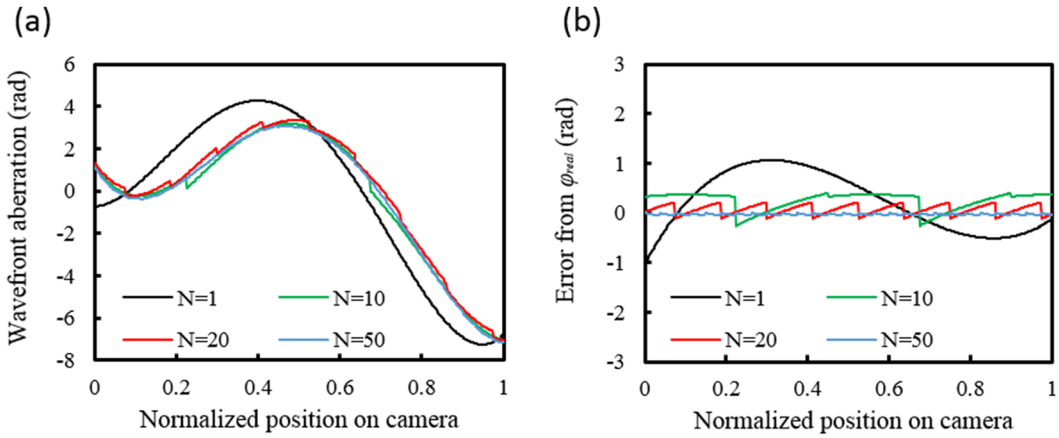

FIG. 5. (a) Simulated wavefront errors with our method. The result at $N = 1$ was taken without scanning. (b) Differences with the real wavefront. The result at $N = 1$ represents the systematic error.

where $\varphi_{real}(m,n)$ and $\varphi_{sys}(m,n)$ are the true wavefront and the systematic error in each pixel, respectively. Here, when moving the camera by certain distance $(a \cdot k)$ equal to k pixels, the measured wavefront can be expressed as

$$\varphi_{meas}(x + a \cdot k, m, n) = \varphi_{real}(m + k, n) + \varphi_{sys}(m, n). \quad (2)$$

Although the object appears to be moving in the field of view of the camera, the object is actually static and the camera is moving. Therefore, formula (2) can also be expressed as

$$\varphi_{meas}(x + a \cdot k, m - k, n) = \varphi_{real}(m, n) + \varphi_{sys}(m - k, n). \quad (3)$$

When this scanning is performed to cover the entire field of view of the camera at one-pixel pitch K times, the summation of all measured wavefronts is expressed as

$$\begin{aligned} S(m,n) &= \sum_k \varphi_{real}(m,n) + \sum_k \varphi_{sys}(m-k,n) \\ &= K \cdot \varphi_{real}(m,n) + constant. \end{aligned} \quad (4)$$

The systematic error term can be constant, which is a meaningless factor for the wavefront. Therefore, it is possible to extract a true wavefront aberration and determine the systematic error of a camera (Fig. 4).

In this method, a camera has to be scanned at one-pixel pitch. The number of measurements exceeds 1000 and it is time consuming. As seen from the differences between the data in Fig. 3, the camera-derived systematic error is assumed to be a slowly curved function. Hence, it is expected that reducing the number of scans does not affect the results.

Simple simulations were carried out to investigate realistic scanning steps. It was assumed that a one-dimensional camera with 400 pixels can directly measure the wavefront aberration and that the camera has a systematic error with a slowly curved shape. Wavefront aberrations estimated using the above method are compared in Fig. 5. Meanwhile, the number of scans of the camera was changed between $N = 1$ (i.e., no scanning) and $N = 50$. In the case of $N = 20$, the calculation error was 0.3 rad (peak-to-valley) on the reconstructed wavefront aberration. Of course, this error gradually decreases with an increase in N, and finally converged to zero at $N = 800$, in which case the scan step is equal to 1 pixel. Therefore, it was found that the condition of $N = 20$ is suitable for practical cases.

V. EXPERIMENTAL RESULTS AND DISCUSSIONS

First, the number of steps in this method was experimentally investigated using X-rays at 9.1 keV at the B29XUL[40] (EH4) of SPring-8. A one-dimensional focusing optical system and a single-grating interferometer, which are the same as the horizontal focusing mirror and the grating interferometer mentioned above, were constructed. The camera motion was controlled by motorized stages with an accuracy of several microns, in which stage-derived systematic errors can be ignored. Wavefront aberrations depending on N were reconstructed using formula (4). Deviations from the averaged data of $N = 50$ and $N = 94$ are shown in Fig. 6. The experimental results were consistent with the simulation results. In the case of $N = 20$, the scanning pitch is 1.56 mm in the horizontal direction and 1.79 mm in the vertical direction.

Next, at the BL 3 (EH5) of SACLA, demonstration experiments were carried out using the optical system shown in Fig. 1. The camera was scanned under the condition of $N = 20$. Systematic-error-free wavefront aberrations were

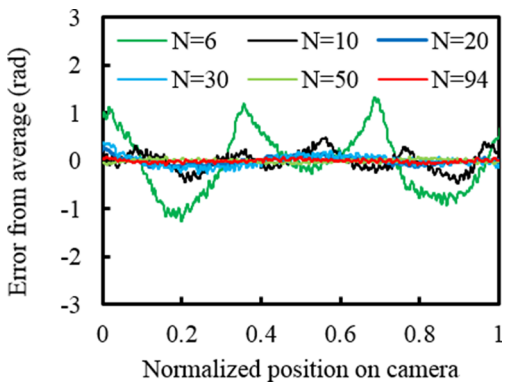

FIG. 6. Reconstructed wavefront aberrations depending on a step number. The data were subtracted from the average obtained using $N = 50$ and $N = 94$.

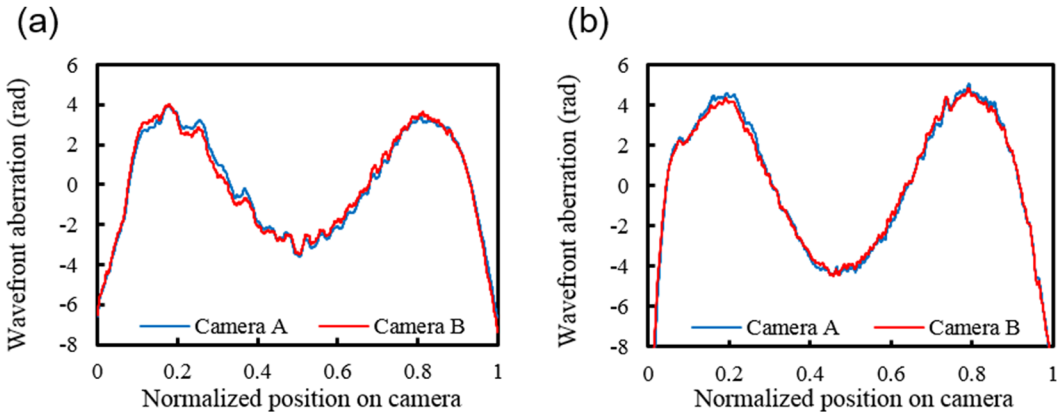

FIG. 7. Wavefront aberration obtained by each camera (after systematic error correction). (a) Vertical and (b) horizontal.

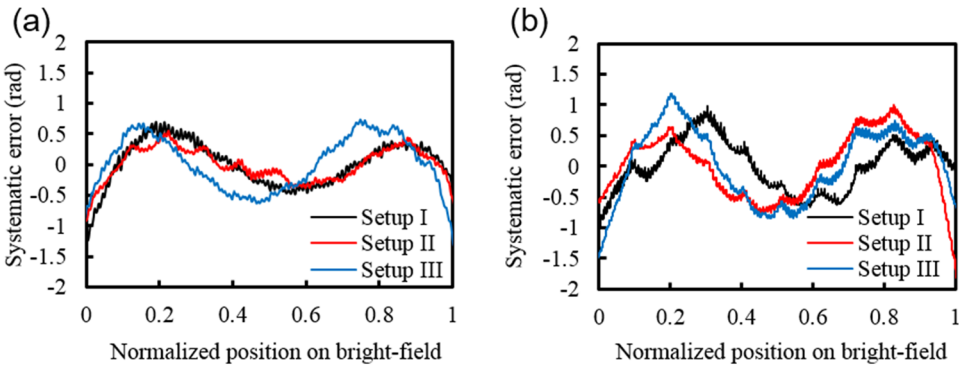

FIG. 8. Systematic errors obtained by each camera setup. The used condition is the same as one in Fig. 7. (a) Vertical and (b) horizontal.

reconstructed using formula (4). The wavefront aberrations obtained by the two different cameras are compared in Fig. 7. The inconsistency between the wavefronts is only 0.5 rad (=λ/12), which is negligibly small to obtain diffraction-limited focusing.

Furthermore, in order to examine the details of the systematic errors, camera setups with different scintillator and detector units, which are the same product model but were manufactured in a different year, are compared in Fig. 8. Setup I is the same camera setup as the one used for Fig. 7. Setups I and II used the same scintillator unit, but a different detector unit. Setups II and III used different scintillator units, but the same detector unit. It was found that even a similar camera setup with the same product models introduced different systematic errors, and therefore error sources exist in the scintillator and detector units.

VI. SUMMARY AND OUTLOOK

In this study, we carefully investigated the systematic errors of a single-grating interferometer based on the Talbot effect. It was found that a grating has no systematic error, but a camera introduced non-negligible systematic errors. In order to overcome the problem, a new method to determine the systematic errors was proposed. Our demonstration experiments confirmed that this method works correctly and can provide wavefront aberrations without systematic errors with an accuracy of less than 0.5 rad.

The method that is used to determine the shape error of a mirror surface will enable us to develop a large-NA multilayer focusing mirror that cannot be fabricated using the conventional techniques. We will proceed to correct the mirror shape with a differential deposition[41] based on the obtained shape error data. When the workflow (wavefront measurement ⇒ shape correction ⇒ perfect focusing) has been established, it is expected that a large-NA multilayer focusing mirror will be available for general users in the future. Applications using synchrotron radiation and XFEL will reach a resolution of less than 10 nm. The combination of large-NA focusing optics and next-generation light sources will allow experiments and discoveries that are currently not feasible.

ACKNOWLEDGMENTS

This research was financially supported by JSPS KAKENHI (Grant Nos. JP23226004, JP16H06358, and JP17H01073), the CREST project of JST, and the JSPS Core-to-Core Program on International Alliance for Material Science in Extreme States with High Power Laser and XFEL. The XFEL experiments were performed at the BL3 of SACLA with the approval of the Japan Synchrotron Radiation Research Institute (JASRI) (Proposal Nos. 2016A8010, 2016B8017, and 2017A8033). Furthermore, the use of B29XUL at the SPring-8 was supported by RIKEN. We are grateful to the SACLA beamline staff and Yoshiki Kohmura of RIKEN for their great help during beam times.

[1]P. Emma, R. Akre, J. Arthur, R. Bionta, C. Bostedt, J. Bozek, A. Brachmann, P. Bucksbaum, R. Coffee, F. J. Decker, Y. Ding, D. Dowell, S. Edstrom, A. Fisher, J. Frisch, S. Gilevich, J. Hastings, G. Hays, P. Hering, Z. Huang, R. Iverson, H. Loos, M. Messerschmidt, A. Miahnahri, S. Moeller, H. D. Nuhn, G. Pile, D. Ratner, J. Rzepiela, D. Schultz, T. Smith, P. Stefan, H. Tompkins, J. Turner, J. Welch, W. White, J. Wu, G. Yocky, and J. Galayda, Nat. Photonics **4**, 641 (2010).

[2]T. Ishikawa, H. Aoyagi, T. Asaka, Y. Asano, N. Azumi, T. Bizen, H. Ego, K. Fukami, T. Fukui, Y. Furukawa, S. Goto, H. Hanaki, T. Hara, T. Hasegawa, T. Hatsui, A. Higashiya, T. Hirono, N. Hosoda, M. Ishii, T. Inagaki, Y. Inubushi, T. Itoga, Y. Joti, M. Kago, T. Kameshima, H. Kimura, Y. Kirihara, A. Kiyomichi, T. Kobayashi, C. Kondo, T. Kudo, H. Maesaka, X. M. Maréchal, T. Masuda, S. Matsubara, T. Matsumoto, T. Matsushita, S. Matsui, M. Nagasono, N. Nariyama, H. Ohashi, T. Ohata, T. Ohshima, S. Ono, Y. Otake, C. Saji, T. Sakurai, T. Sato, K. Sawada, T. Seike, K. Shirasawa, T. Sugimoto, S. Suzuki, S. Takahashi, H. Takebe, K. Takeshita, K. Tamasaku, H. Tanaka, R. Tanaka, T. Tanaka, T. Togashi, K. Togawa, A. Tokuhisa, H. Tomizawa, K. Tono, S. Wu, M. Yabashi, M. Yamaga, A. Yamashita, K. Yanagida, C. Zhang, T. Shintake, H. Kitamura, and N. Kumagai, Nat. Photonics **6**, 540 (2012).

[3]C. G. Schroer, O. Kurapova, J. Patommel, P. Boye, J. Feldkamp, B. Lengeler, M. Burghammer, C. Riekel, L. Vincze, A. van der Hart, and M. Küchler, Appl. Phys. Lett. **87**, 124103 (2005).

[4]T.-Y. Chen, Y.-T. Chen, C.-L. Wang, I. M. Kempson, W.-K. Lee, Y. S. Chu, Y. Hwu, and G. Margaritondo, Opt. Express **19**, 19919 (2011).

[5]H. C. Kang, H. Yan, R. P. Winarski, M. V. Holt, J. Maser, C. Liu, R. Conley, S. Vogt, A. T. MacRander, and G. B. Stephenson, Appl. Phys. Lett. **92**, 221114 (2008).

[6]H. Mimura, H. Yumoto, S. Matsuyama, Y. Sano, K. Yamamura, Y. Mori, M. Yabashi, Y. Nishino, K. Tamasaku, T. Ishikawa, and K. Yamauchi, Appl. Phys. Lett. **90**, 051903 (2007).

[7]O. Hignette, P. Cloetens, G. Rostaing, P. Bernard, and C. Morawe, Rev. Sci. Instrum. **76**, 063709 (2005).

[8]G. E. Ice, J. S. Chung, J. Z. Tischler, A. Lunt, and L. Assoufid, Rev. Sci. Instrum. **71**, 2635 (2000).

[9]J. Cesar da Silva, A. Pacureanu, Y. Yang, S. Bohic, C. Morawe, R. Barrett, and P. Cloetens, Optica **4**, 492 (2017).

[10]H. Mimura, S. Handa, T. Kimura, H. Yumoto, D. Yamakawa, H. Yokoyama, S. Matsuyama, K. Inagaki, K. Yamamura, Y. Sano, K. Tamasaku, Y. Nishino, M. Yabashi, T. Ishikawa, and K. Yamauchi, Nat. Phys. **6**, 122 (2010).

[11]C. David, S. Gorelick, S. Rutishauser, J. Krzywinski, J. Vila-Comamala, V. A. Guzenko, O. Bunk, E. Färm, M. Ritala, M. Cammarata, D. M. Fritz, R. Barrett, L. Samoylova, J. Grünert, and H. Sinn, Sci. Rep. **1**, 57 (2011).

[12]H. Mimura, S. Morita, T. Kimura, D. Yamakawa, W. Lin, Y. Uehara, S. Matsuyama, H. Yumoto, H. Ohashi, K. Tamasaku, Y. Nishino, M. Yabashi, T. Ishikawa, H. Ohmori, and K. Yamauchi, Rev. Sci. Instrum. **79**, 083104 (2008).

[13]K. Yamauchi, H. Mimura, K. Inagaki, and Y. Mori, Rev. Sci. Instrum. **73**, 4028 (2002).

[14]A. Shorey, W. Kordonski, and M. Tricard, Proc. SPIE **5533**, 99 (2004).

[15]T. Arnold, G. Böhm, R. Fechner, J. Meister, A. Nickel, F. Frost, T. Hänsel, and A. Schindler, Nucl. Instrum. Methods Phys. Res., Sect. A **616**, 147 (2010).

[16]K. Yamauchi, K. Yamamura, H. Mimura, Y. Sano, A. Saito, K. Ueno, K. Endo, A. Souvorov, M. Yabashi, K. Tamasaku, T. Ishikawa, and Y. Morib, Rev. Sci. Instrum. **74**, 2894 (2003).

[17]H. Mimura, H. Yumoto, S. Matsuyama, K. Yamamura, Y. Sano, K. Ueno, K. Endo, Y. Mori, M. Yabashi, K. Tamasaku, Y. Nishino, T. Ishikawa, and K. Yamauchi, Rev. Sci. Instrum. **76**, 045102 (2005).

[18]F. Siewert, H. Lammert, T. Noll, T. Schlegel, T. Zeschke, T. Hänsel, A. Nickel, A. Schindler, B. Grubert, and C. Schlewitt, Proc. SPIE **5921**, 592101 (2005).

[19]S. G. Alcock, K. J. S. Sawhney, S. Scott, U. Pedersen, R. Walton, F. Siewert, T. Zeschke, F. Senf, T. Noll, and H. Lammert, Nucl. Instrum. Methods Phys. Res., Sect. A **616**, 224 (2010).

[20]K. Yamauchi, H. Mimura, T. Kimura, H. Yumoto, S. Handa, S. Matsuyama, K. Arima, Y. Sano, K. Yamamura, K. Inagaki, H. Nakamori, J. Kim, K. Tamasaku, Y. Nishino, M. Yabashi, and T. Ishikawa, J. Phys.: Condens. Matter **23**, 394206 (2011).

[21]J. P. Sutter, S. G. Alcock, and K. Sawhney, Nucl. Instrum. Methods Phys. Res., Sect. A **710**, 72 (2013).

[22]T. Kimura, H. Mimura, S. Handa, H. Yumoto, H. Yokoyama, S. Imai, S. Matsuyama, Y. Sano, K. Tamasaku, Y. Komura, Y. Nishino, M. Yabashi, T. Ishikawa, and K. Yamauchi, Rev. Sci. Instrum. **81**, 123704 (2010).

[23]Y. Kashyap, H. Wang, and K. Sawhney, Rev. Sci. Instrum. **87**, 052001 (2016).

[24]A. Schropp, P. Boye, J. M. Feldkamp, R. Hoppe, J. Patommel, D. Samberg, S. Stephan, K. Giewekemeyer, R. N. Wilke, T. Salditt, J. Gulden, A. P. Mancuso, I. A. Vartanyants, E. Weckert, S. Schöder, M. Burghammer, and C. G. Schroer, Appl. Phys. Lett. **96**, 091102 (2010).

[25]C. M. Kewish, M. Guizar-Sicairos, C. Liu, J. Qian, B. Shi, C. Benson, A. M. Khounsary, J. Vila-Comamala, O. Bunk, J. R. Fienup, A. T. Macrander, and L. Assoufid, Opt. Express **18**, 23420 (2010).

[26]M. Idir, P. Mercere, M. H. Modi, G. Dovillaire, X. Levecq, S. Bucourt, L. Escolano, and P. Sauvageot, Nucl. Instrum. Methods Phys. Res., Sect. A **616**, 162 (2010).

[27]S. Rutishauser, I. Zanette, T. Weitkamp, T. Donath, and C. David, Appl. Phys. Lett. **99**, 221104 (2011).

[28]S. Matsuyama, H. Yokoyama, R. Fukui, Y. Kohmura, K. Tamasaku, M. Yabashi, W. Yashiro, A. Momose, T. Ishikawa, and K. Yamauchi, Opt. Express **20**, 24977 (2012).

[29]H. F. Talbot, Philos. Mag. **9**, 401 (1836).

[30]Y. Takeda, W. Yashiro, Y. Suzuki, S. Aoki, T. Hattori, and A. Momose, Jpn. J. Appl. Phys., Part 2 **46**, L89 (2007).

[31]K. Tono, T. Kudo, M. Yabashi, T. Tachibana, Y. Feng, D. Fritz, J. Hastings, and T. Ishikawa, Rev. Sci. Instrum. **82**, 023108 (2011).

[32]Y. Kayser, C. David, U. Flechsig, J. Krempasky, V. Schlott, and R. Abela, J. Synchrotron Radiat. **24**, 150 (2017).

[33]Y. Inubushi, I. Inoue, J. Kim, A. Nishihara, S. Matsuyama, H. Yumoto, T. Koyama, K. Tono, H. Ohashi, K. Yamauchi, and M. Yabashi, Appl. Sci. **7**, 584 (2017).

[34]P. Kirkpatrick and A. V. Baez, J. Opt. Soc. Am. **38**, 766 (1948).

[35]H. Mimura, H. Yumoto, S. Matsuyama, T. Koyama, K. Tono, Y. Inubushi, T. Togashi, T. Sato, J. Kim, R. Fukui, Y. Sano, M. Yabashi, H. Ohashi, T. Ishikawa, and K. Yamauchi, Nat. Commun. **5**, 3539 (2014).

[36]J. Kim, H. Yokoyama, S. Matsuyama, Y. Sano, and K. Yamauchi, Curr. Appl. Phys. **12**, S20 (2012).

[37]A. Momose, S. Kawamoto, I. Koyama, Y. Hamaishi, K. Takai, and Y. Suzuki, Jpn. J. Appl. Phys., Part 2 **42**, L866 (2003).

[38]R. Fukui, J. Kim, S. Matsuyama, H. Yumoto, Y. Inubushi, K. Tono, T. Koyama, T. Kimura, H. Mimura, H. Ohashi, M. Yabashi, T. Ishikawa, and K. Yamauchi, Synchrotron Radiat. News **26**, 13 (2013).

[39]M. Born and E. Wolf, *Principles of Optics*, 7th ed. (Cambridge University Press, 1999), pp. 421–425.

[40]K. Tamasaku, Y. Tanaka, M. Yabashi, H. Yamazaki, N. Kawamura, M. Suzuki, and T. Ishikawa, Nucl. Instrum. Methods Phys. Res., Sect. A **467-468**, 686 (2001).

[41]S. Handa, H. Mimura, H. Yumoto, T. Kimura, S. Matsuyama, Y. Sano, and K. Yamauchi, Surf. Interface Anal. **40**, 1019 (2008).